

## Supporting Information

### Hydrogen Spillover Enhancing the Alkaline Hydrogen Electrocatalysis on Interface-Rich Metallic Pt-Supported MoO<sub>3</sub>

Rajib Samanta,<sup>#a,b</sup> Biplab Kumar Manna,<sup>#a,b</sup> Ravi Trivedi,<sup>c,d</sup> Brahmananda Chakraborty,<sup>b,e</sup> and Sudip Barman<sup>\*a,b</sup>

<sup>a</sup> School of Chemical Sciences, National Institute of Science Education and Research (NISER), HBNI, Bhubaneswar, Orissa-752050, India, Tel.: +91 6742494183.

<sup>b</sup> Homi Bhabha National Institute, Training School Complex, Anushakti Nagar, Mumbai - 400094, India.

<sup>c</sup> Department of Physics, Karpagam Academy of Higher Education, Coimbatore, India – 641021.

<sup>d</sup> Centre for High Energy Physics, Karpagam Academy of Higher Education, Coimbatore, India. 641021

<sup>e</sup> High Pressure Synchrotron Radiation Physics Division, Bhabha Atomic Research Centre, Trombay, Mumbai-400085, India.

\*S.B.: E-mail - sbarman@niser.ac.in; Tel: +91(674)2494183.

# Authors with equal contributions;

#### Materials:

Chloroplatinic acid (H<sub>2</sub>PtCl<sub>6</sub> · 6H<sub>2</sub>O), formamide (HCONH<sub>2</sub>), platinum supported on carbon (Pt/C), and Molybdenum (V) pent-chloride (MoCl<sub>5</sub>, 99%), were purchased from Sigma-Aldrich. Sodium borohydride (NaBH<sub>4</sub>) was brought from Spectrochem (India). We purchased perchloric acid (HClO<sub>4</sub>), acetic acid (CH<sub>3</sub>COOH, 99%), sodium acetate (CH<sub>3</sub>COONa), boric acid (H<sub>3</sub>BO<sub>3</sub>), potassium carbonate (K<sub>2</sub>CO<sub>3</sub>), potassium bicarbonate (KHCO<sub>3</sub>), and potassium hydroxide (KOH) from Merck. All the chemicals were used without further purification as they were received. The N<sub>2</sub>, H<sub>2</sub>, and CO gases were obtained from Sigma Aldrich at a purity of 99.99%. An ultra-filtration system (Mili-Q, Millipore) was used to obtain Mili-Q water with a conductivity of 28 mho.cm<sup>-1</sup> at 25 °C.

## **Experimental Section:**

### **Preparation of Nitrogen-doped Carbon (CN<sub>x</sub>):**

Previously, our group reported the synthesis of nitrogen-doped carbon using microwave irradiation of formamide (HCONH<sub>2</sub>) at 180 °C. The microwave irradiation of 30 mL HCONH<sub>2</sub> at 180 °C was conducted for 3 hours. As a result, a brown-colored solution appeared. Then, a rotary evaporator was used at 180 °C to evaporate the unreacted formamide to form nitrogen-doped carbon. Ultimately, the product was filtered and thoroughly washed with distilled water, and then vacuum dried to form a solid, dry nitrogen-doped carbon product.

### **Preparation of PtMo/CN<sub>x</sub> and Pt/MoO<sub>3</sub>-CN<sub>x</sub>-400 Composite:**

The Pt/MoO<sub>3</sub>-CN<sub>x</sub> composite was formed by two simple steps. First, 20 mg of molybdenum (V) Chloride (MoCl<sub>5</sub>) and 13 mg of Chloroplatinic acid (H<sub>2</sub>PtCl<sub>6</sub> · 6H<sub>2</sub>O) were mixed in 6 mL de-ionized water followed by ultrasonic treatment. In another beaker, 5 mg of as-prepared CN<sub>x</sub> was taken and dispersed in 2 mL water by sonication using a bath sonicator (60 Hz frequency) for 10 minutes. Then two solutions are mixed and sonicated for 30 minutes. After that, 1 mL solution containing 60 mg of NaBH<sub>4</sub> was added to the mixed solution under continuous sonication. At last, the resultant black solution was sonicated in bath sonication for 2 hours under 60 Hz frequencies. A black mass precipitated out from the solution after ultrasound treatment. The black precipitate was collected by centrifugation at 10000 rpm for 5 minutes and washed with de-ionized water & ethanol repeatedly. Then the product was kept in a vacuum for drying. The product was named as PtMo/CN<sub>x</sub>.

In the second step, the PtMo/CN<sub>x</sub> was calcinated at 400 °C for 3 hours in a muffle furnace with a temperature accuracy of ± 2 °C to form Pt/MoO<sub>3</sub>-CN<sub>x</sub>. Then, it was cooled down to room temperature normally & a black solid product was collected carefully. The formed compound was named as Pt/MoO<sub>3</sub>-CN<sub>x</sub>-400. The Pt/MoO<sub>3</sub>-CN<sub>x</sub>-350 and Pt/MoO<sub>3</sub>-CN<sub>x</sub>-450 was also prepared by the calcination of PtMo/CN<sub>x</sub> at 350 and 450 °C, respectively. The Pt/MoO<sub>3</sub>-CN<sub>x</sub>-400 with different Pt and Mo ratio was also synthesized by changing the amount of Pt and Mo salt by the same synthesis procedure. Pt/MoO<sub>3</sub>-400 was also prepared by the same synthesis method without adding CN<sub>x</sub> and heating the sample at 400 °C temperature in presence of air.

### **Preparation of Mo/CN<sub>x</sub>-400 Composite:**

At first, Mo/CN<sub>x</sub> was prepared by the same NaBH<sub>4</sub> treatment of 30 mg MoCl<sub>5</sub> and 5 mg CN<sub>x</sub> mixture in 8 mL of DI water. After that, Mo/CN<sub>x</sub>-400 was prepared by the calcination of as-prepared Mo/CN<sub>x</sub> at 400 °C temperature for 3 hours in muffle furnace in presence of air.

### **Preparation of Pt/CN<sub>x</sub>-400 Composite:**

Firstly, Pt/CN<sub>x</sub> was synthesized by the NaBH<sub>4</sub> treatment of 30 mg H<sub>2</sub>PtCl<sub>6</sub>.6H<sub>2</sub>O and 5 mg CN<sub>x</sub> mixture in 8 mL of DI water. After that, Pt/CN<sub>x</sub> was calcinated at 400 °C temperature for 3 hours in muffle furnace in presence of air to form Pt/CN<sub>x</sub>-400.

### **Characterizations:**

MAS-II microwave synthesizer bought from Shanghai SINEO Microwave Technology Company (China) was used to synthesize CN<sub>x</sub>. The sonication was carried out by an Ultrasound Bath Sonicator, developed by Genei Laboratories Private Limited, Bangalore, India. To capture FESEM images, a Carl Zeiss FESEM (model sigma, Germany, made by Carl Zeiss) was used. A drop of the FESEM solution was cast on a silicon wafer, and the samples were dried in the air at 45°C. The powder x-ray diffraction pattern (p-XRD) of the samples was performed by a Bruker DAVINCI D8 ADVANCE diffractometer equipped with Cu K<sub>α</sub> radiation (λ= 0.15406 nm). Transmission Electron Microscopy (TEM, JEOL F200) operated at 200 kV, was used to investigate surface morphology along with High-Resolution TEM (HRTEM) images. For TEM sample preparation, 10 μl of the solution of 4 x10<sup>-5</sup> mg/l was taken and dried at 45 °C. Mg K<sub>α</sub> X-rays were used as the monochromatic source for the XPS measurements performed by VG Microtech. An XPS sample was taken from a Si-wafer deposited with the sample. Each electrochemical measurement was carried out on an Electrochemical Workstation (Autolab, Metrohm, PGSTAT 320N) fitted with a rotating disk electrode (RDE). The experimental setup utilized a conventional 3-electrode system, consisting of a platinum electrode, a glassy carbon electrode, and an Ag/AgCl electrode for the reference electrode. A Hanna (HI 2209) pH meter was used to measure pH before the experiment.

### **Electrochemical measurements:**

An Autolab 302 N electrochemical station is used to perform all electrochemical measurements, using glassy carbon (GC) as a working electrode, Pt wire as a counter electrode, and Ag/AgCl (3M KCl) as a reference electrode. On Buehler micro cloth polishing cloth, 1.0, 0.1-, and 0.05-mm alumina slurry was used to polish the working GC electrode. It was then washed with copious amounts of water and sonicated in distilled water for a few minutes. The synthesized composite was dissolved in 1 mL of water to make a stock solution. We prepared the Pt/MoO<sub>3</sub>-CN<sub>x</sub> electrode by drop-casting and evaporating 2.5 μL of the aqueous stock solution onto a clean glassy carbon electrode. The amount of PtMo on the GC electrode was 23.93 μg/cm<sup>2</sup>. For stability measurement, 5 μL 5 wt% Nafion solutions were used to make the stock solution. 5 μL of aqueous stock solution (i.e. 48 μg/cm<sup>2</sup> of PtMo) was evaporated on GC for chronopotentiometric study in KOH medium. For comparison, we used 40 wt% commercial Pt/C and the amount of Pt loading of comm. Pt/C was also kept the same as Pt/MoO<sub>3</sub>-CN<sub>x</sub>-400 for comparison. 10 μL ethanol and 10 μL 5% Nafion were used to make the stock solution of comm Pt/C. By using the general formula  $E_{\text{RHE}} = E_{\text{Ag/AgCl}} + E^{\circ}_{\text{Ag/AgCl}} + (0.059 * \text{pH})$ , potential obtained from Ag/AgCl reference electrode was converted to RHE, where  $E^{\circ}_{\text{Ag/AgCl}} = 0.1976$  at 25 °C (3 M KCl) and  $E_{\text{Ag/AgCl}}$  is the working potential. Before the experiment, pH was also measured for all electrolytes and the HER measurements were carried out in both basic and acidic mediums after degassing with nitrogen using LSV at a scan rate of 5 mV/sec. HOR in different pH solutions was done in an H<sub>2</sub>-saturated environment with the help of linear sweep voltammetry (LSV) at a scan rate of 10 mV sec<sup>-1</sup> scan rate. For CV in different pH, 30 mV/sec scan rate was used with N<sub>2</sub> saturated medium. In CO stripping measurement, for full monolayer adsorption of CO on the metal surface, first, the electrode potential was held at 0.1V (RHE). Then N<sub>2</sub> was flowed for some minutes to remove the dissolved CO from the solution. After that, a CV scan was performed at 30 mV/sec where the forward scan represents the CO stripping. The stability of the electrode was measured by chronopotentiometric measurement by applying a constant current for a certain time. AC impedance measurements were performed in the identical system with a constant AC voltage in the frequency range 10<sup>5</sup> Hz to 10<sup>-1</sup> Hz. Cell (solution) resistance was calculated by linearly extrapolating the intercept of impedance spectra with the real axis, and this value was used for iR correction. All HOR polarization curves in different pH were iR corrected.

### **Electrochemically active surface area (ECSA) calculation:**

Electrochemically active surface area (ECSA) was determined by the following equation:

$$\text{ECSA} = S/m \times v \times c$$

Where S is double layer corrected total area under CO stripping curve, m is the Pt loading on the electrode surface (mg), v is the scan rate (V/s) and c is the required charge to oxidize a monolayer of CO on the platinum molybdenum oxide surface ( $\text{mC}\cdot\text{cm}^{-2}$ ). The value of c is  $0.42 \text{ mC}\cdot\text{cm}^{-2}$  for CO stripping.

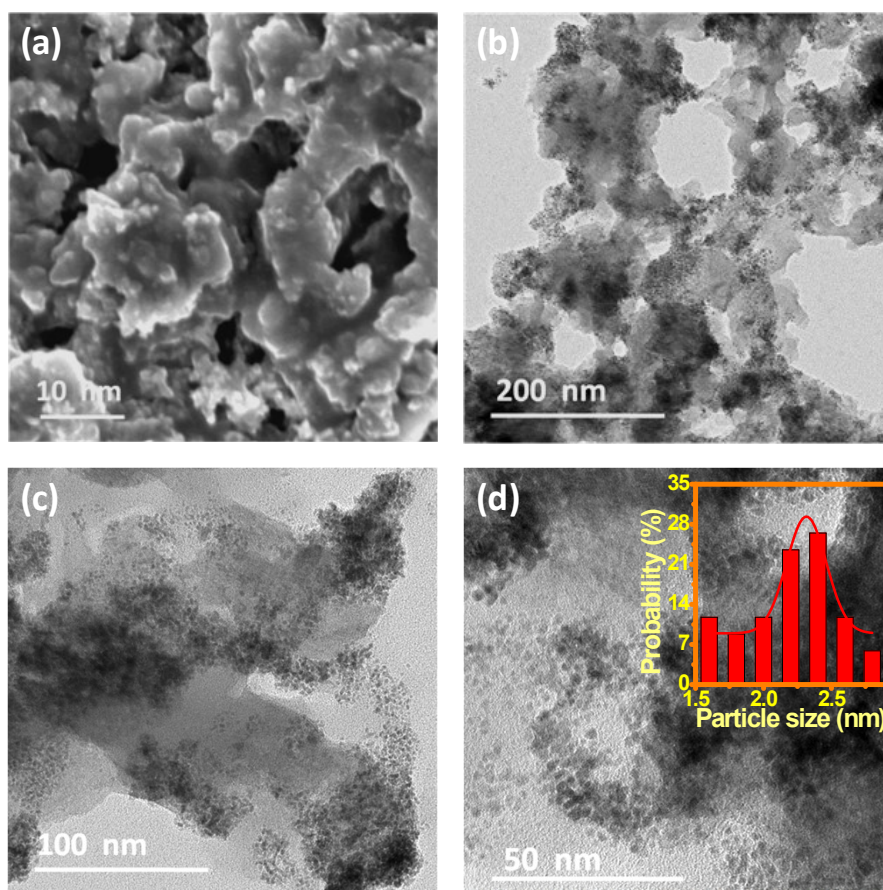


**Figure S1.** (a) FESEM image, (b-d) TEM images of PtMo/CN<sub>x</sub> (Inset Figure S1d: particle size distribution plot).

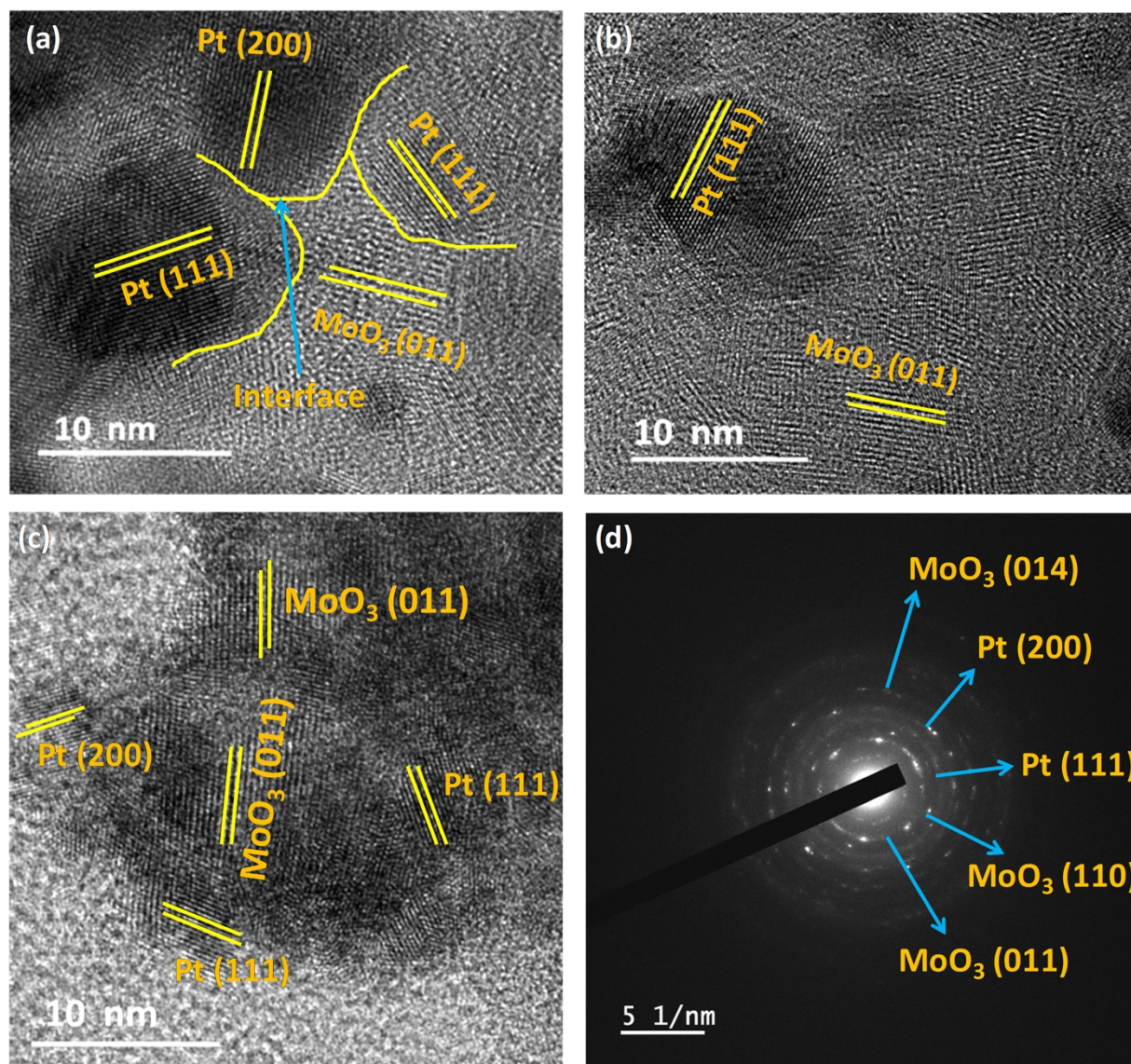


**Figure S2.** (a, b) HRTEM images of Pt/MoO<sub>3</sub>-CN<sub>x</sub>-400; (c, d) HRTEM and SAED images of PtMo/CN<sub>x</sub>, respectively.

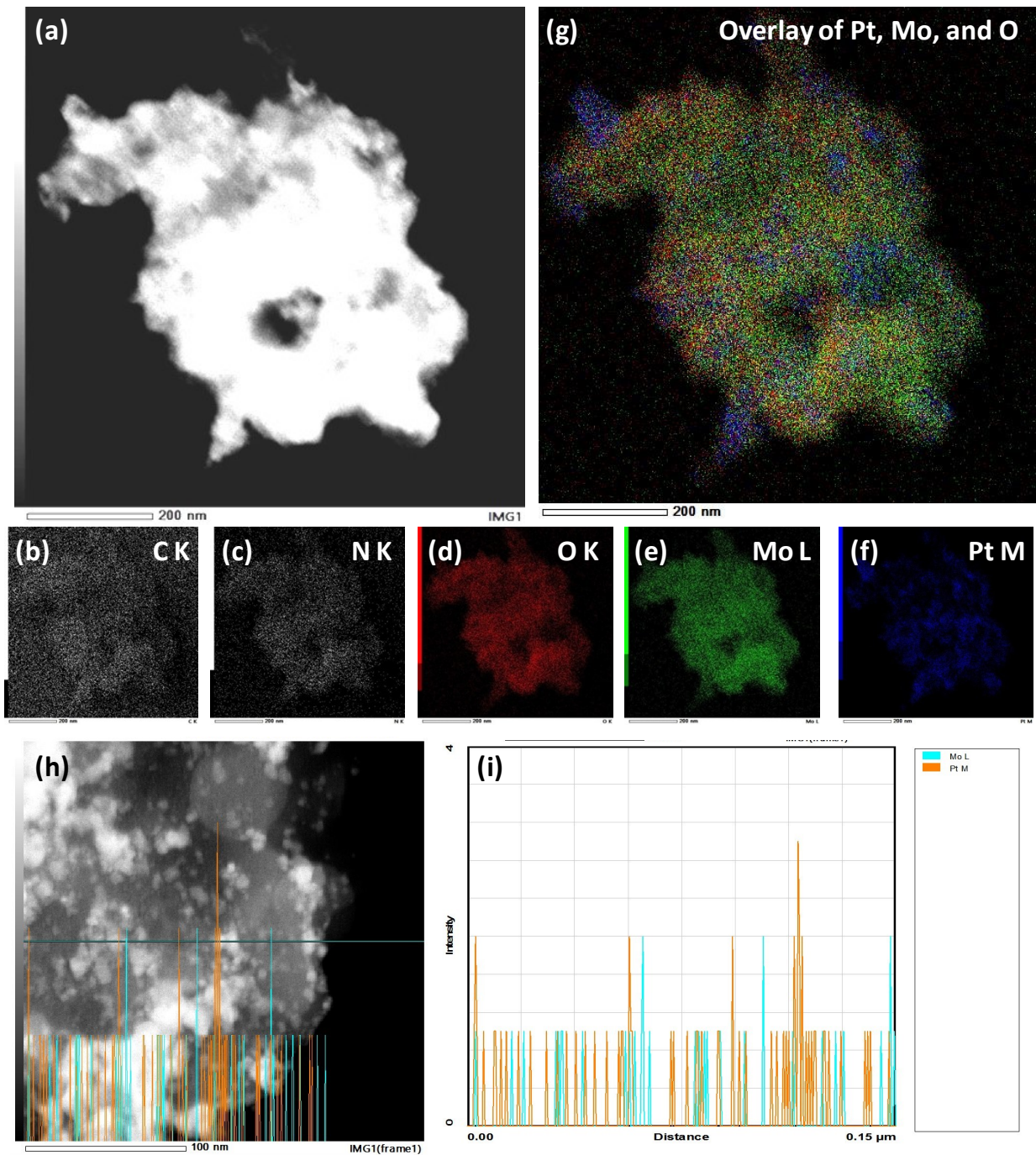


**Figure S3.** (a-f) STEM image and the corresponding elemental mapping images of PtMo/CN<sub>x</sub>; (g) elemental overlapping image of Pt, Mo, and O of PtMo/CN<sub>x</sub>. (h, i) Line scan profile of Pt and Mo on Pt/MoO<sub>3</sub>-CN<sub>x</sub>-400.

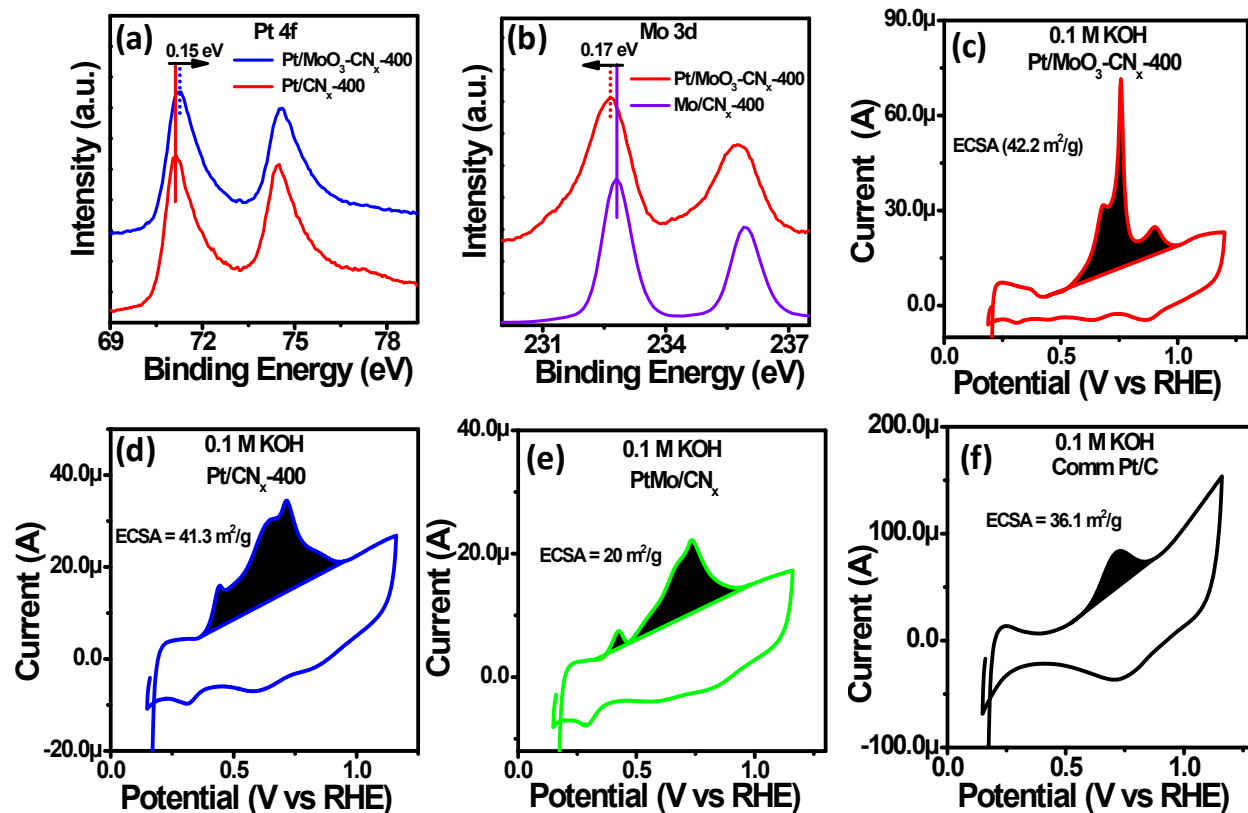


**Figure S4.** (a) Comparison of Pt 4f XPS spectra of Pt/MoO<sub>3</sub>-CN<sub>x</sub>-400 and Pt/CN<sub>x</sub>-400; (b) Comparison of Mo 3d XPS spectra of Pt/MoO<sub>3</sub>-CN<sub>x</sub>-400 and Mo/CN<sub>x</sub>-400. CO-stripping experiment of (c) Pt/MoO<sub>3</sub>-CN<sub>x</sub>-400, (d) Pt/CN<sub>x</sub>-400, (e) PtMo/CN<sub>x</sub>, (f) comm Pt/C in base, respectively.

**Table S1.** The weight percentage of the metals present in the compounds by ICP-OES measurements.

Compound	Weight % of Pt	Weight % of Mo	Metal ratio (Pt : Mo)
Pt/MoO <sub>3</sub> -CN <sub>x</sub> -400	~ 20	~ 26	~ 1 : 1.3
PtMo/CN <sub>x</sub>	~ 14.7	~ 40	~ 1 : 2.7
Pt/CN <sub>x</sub> -400	78	-----	-----
Mo/CN <sub>x</sub> -400	-----	46	-----

### **Tafel plot:**

The linear region of the Tafel plots is fitted using the Tafel formula:  $\eta = b \log (J) + a$ , where ‘ $\eta$ ’, ‘ $J$ ’, ‘ $b$ ’, and ‘ $a$ ’ is overpotential, current density, Tafel slope, and constant respectively.

Where,  $b = 2.3RT/\alpha F$  ( $R$  - gas constant,  $\alpha$  - symmetry coefficient,  $T$  - absolute temperature,  $F$  - faraday constant). The lower value of the Tafel slope ( $b$ ) indicates the faster electron transfer during the electrochemical process.

### **Hydrogen evolution reaction (HER) mechanism:**

Hydrogen evolution reaction undergoes two different reaction mechanisms under acid and alkaline medium in three steps. One of the mechanisms is Volmer-Heyrovsky, and another is Volmer-Tafel, in which Volmer is the primary discharge step common in both mechanisms.

#### **HER mechanism in alkaline medium**

(1)  $H_2O + e^- + AS \rightleftharpoons AS-H_{ad} + OH^-$ ; Volmer Step (Discharge Step)

(2)  $H_2O + e^- + AS-H_{ad} \rightleftharpoons AS + H_2 + OH^-$ ; Heyrovsky reaction (Electrochemical desorption step)

(3)  $AS-H_{ad} + H_{ad}-AS \rightleftharpoons H_2 + 2AS$ ; Tafel reaction (Recombination Step).

The rate-determining step, or the slowest step in the HER process, depends on the affinity between intermediates and the metal surface. If the bonding between the catalyst and hydrogen intermediate is weak, then the whole reaction is dominated by the Volmer step. If the bonding strength between the catalyst surface and hydrogen intermediates is very strong, then the Heyrovsky or Tafel would be the rate-limiting dominating step. It is required to get moderate bonding between the catalyst and hydrogen intermediate to facilitate the adsorption and desorption process to produce  $H_2$  molecules.

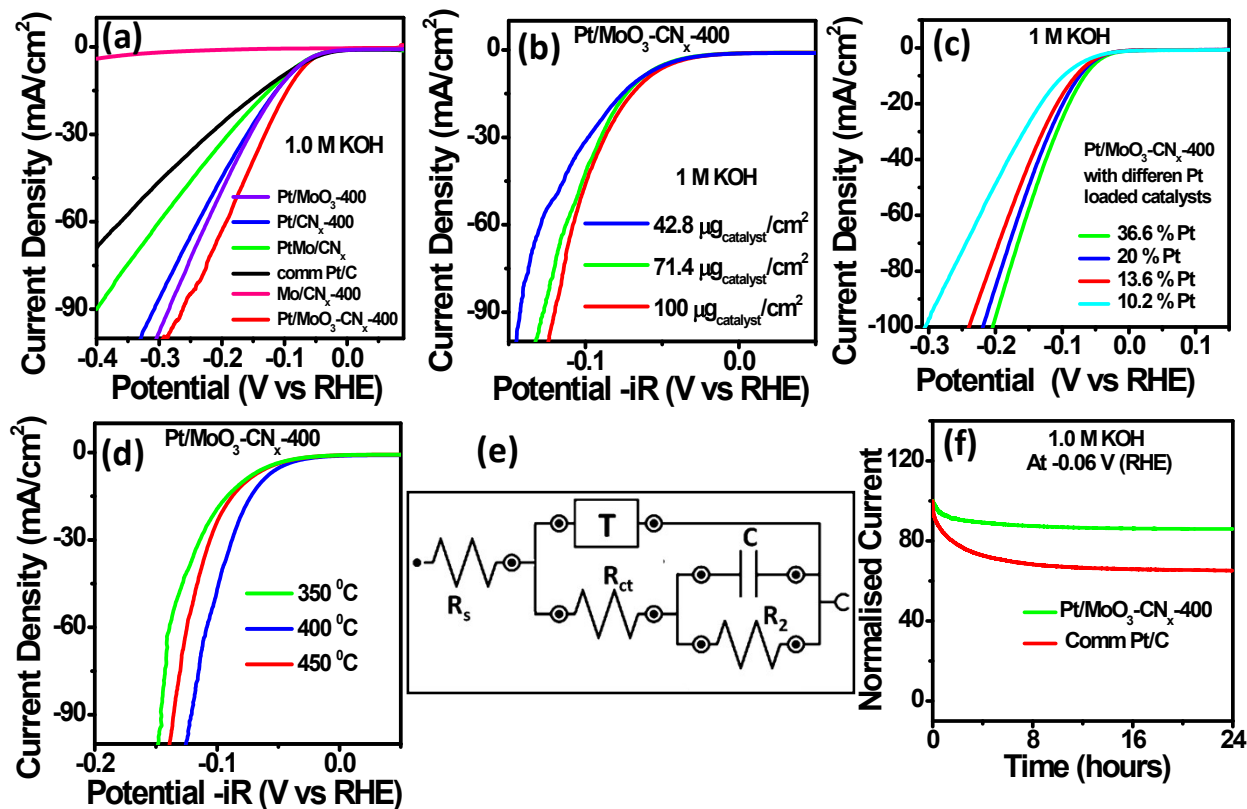


**Figure S5.** (a) Non-iR-corrected HER plots of Pt/MoO<sub>3</sub>-CN<sub>x</sub>-400, Pt/CN<sub>x</sub>-400, Pt/MoO<sub>3</sub>-400, Mo/CN<sub>x</sub>-400, comm Pt/C, and PtMo/CN<sub>x</sub> in base, (b-d) HER polarization curves of Pt/MoO<sub>3</sub>-CN<sub>x</sub>-400 with different loading, different Pt and Mo ratios, and different synthesis temperature, respectively; (e) equivalent circuit for fitting of Nyquist plots; (f) HER stability test of Pt/MoO<sub>3</sub>-CN<sub>x</sub>-400, and commercial Pt/C in presence of nafion binder.

**Table S2.** Comparison of HER activity parameters of Pt/MoO<sub>3</sub>-CN<sub>x</sub>-400 with other catalysts in the base.

Catalyst	Solution	Overpotential (mV) at 10 mA/cm <sup>2</sup>	Current density at -0.1 V (RHE) (mA/cm <sup>2</sup> )	Mass Activity at -0.1 V (RHE) (mA/mg <sub>metal</sub> )	Surface Activity at -0.1 V (RHE) (mA/cm <sup>2</sup> <sub>metal</sub> )	Tafel Slope (mV/dec)
Pt/MoO <sub>3</sub> -CN <sub>x</sub> -400	1.0 M KOH	66.8	50.2	3514	8.327	41.2
Pt/MoO <sub>3</sub> -400	1.0 M KOH	76.7	22.57	1580.2	3.76	64.3
PtMo/CN <sub>x</sub>	1.0 M KOH	88	13.24	926.8	4.63	63.2
Pt/CN <sub>x</sub> -400	1.0 M KOH	80.2	19.2	1344	3.25	52.7
Commercial Pt/C	1.0 M KOH	93.4	11.2	784	2.17	82.6

**Table S3:** Comparison of HER activity of Pt/MoO<sub>3</sub>-CN<sub>x</sub>-400 catalyst in alkaline medium with other reported catalysts.

Catalyst	Electrolyte	Loading (μg/cm <sup>2</sup> )	Overpotential at 10 mA/cm <sup>2</sup> current density	Tafel slope (mV/dec)	References
NiRu <sub>0.13</sub> -BDC	1.0M KOH	2500	34		Nat. Commun. 2021, 12, 1369
PtRu NCs/BP	1.0M KOH	14.8	22	19	ACS Catal. 2019, 9, 10870–10875
PdNi-S/C	1.0M KOH	-	67	69.4	ACS Appl. Mater. Interfaces 2020, 12, 2, 2243–2251
Pt <sub>3</sub> Ni <sub>2</sub> NWs-S/C	1.0M KOH	15.3	50	-	Nat. Commun. 2017, 8, 14580
Ru/Co <sub>3</sub> O <sub>4</sub> NWs	1.0M KOH	354	31		Nano Energy 2021, 85,105940
Ru <sub>x</sub> Se-400	1.0M KOH	-	45	31.4	Nanoscale, 2020,12, 23740-23747
Ag-Ni <sub>3</sub> S <sub>2</sub> /NF	1.0M KOH		89	90	Nanoscale, 2020,12, 19333-19339
P-Ru/C	1.0M KOH	30	31	105	ACS Catal. 2020, 10, 11751–11757
Pt NWs/SL Ni(OH) <sub>2</sub>	1.0M KOH	16	65		Nat. Commun. 2015, 6, 6430
IrP <sub>2</sub> @NPC	1.0M KOH	200	42		J. Mater. Chem. A 2021, 9, 2195-2204
Pt-Co(OH) <sub>2</sub> /CC	1.0M KOH	390	32	70	ACS Catalysis, 2017, 7, 7131
Porous Pd-CN <sub>x</sub>	1.0M KOH	43	180	150	ACS Catal.2016,6, 1929
Ru-MnFeP/NF	1.0M KOH		35		Adv. Energy Mater. 2020, 10, 2000814
PtNi-O	1.0M KOH	5.1	39.8	78.8	J. Am. Chem. Soc., 2018, 140, 9046.
1D-RuO <sub>2</sub> -CN <sub>x</sub>	1.0M KOH	12	95	70	ACS Appl. Mater. Interfaces 2016, 8 (42), 28678.
Rh nanosheets	1.0M KOH	15	37	74.7	Chem. Mater. 2017, 29, 5009.
PdO-RuO <sub>2</sub> /C	1.0M KOH	17.8	44	34	ChemSusChem 2021, 14, 2112–2125
<b>Pt/MoO<sub>3</sub>-CN<sub>x</sub>-400</b>	<b>1.0M KOH</b>	<b>14.28</b>	<b>66.8</b>	<b>41.2</b>	<b>This Work</b>

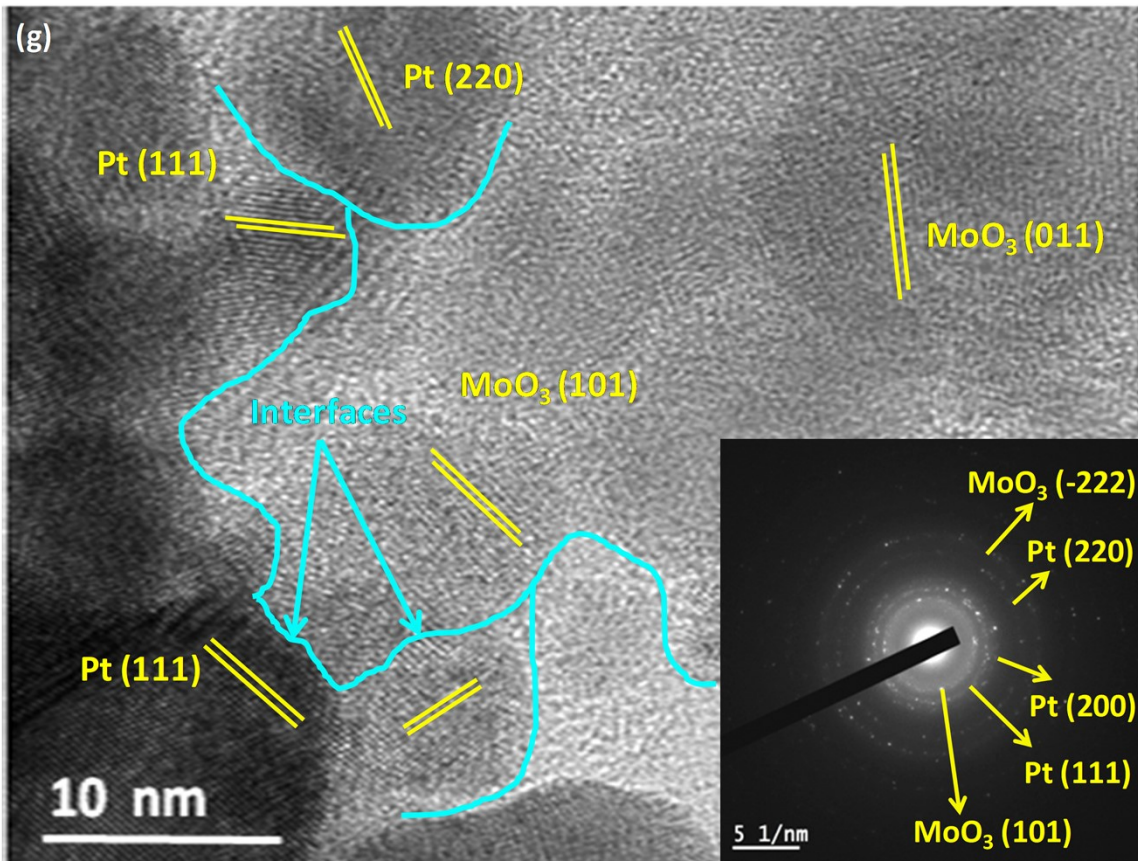
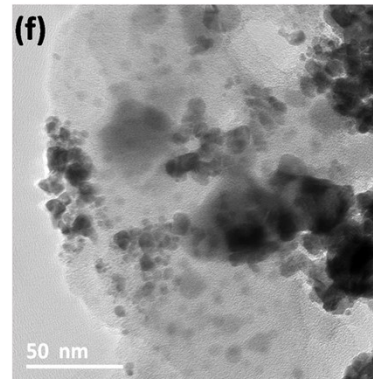
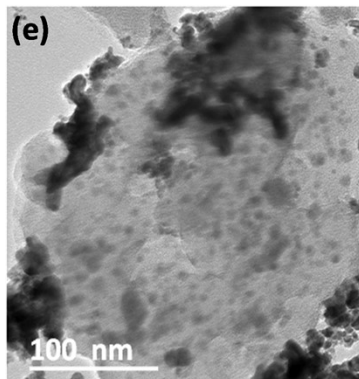
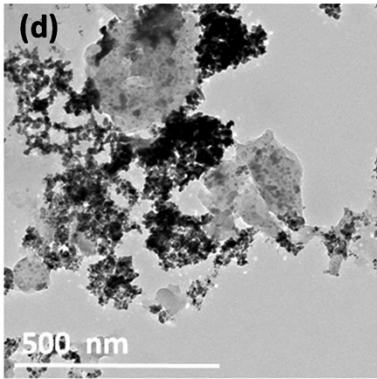
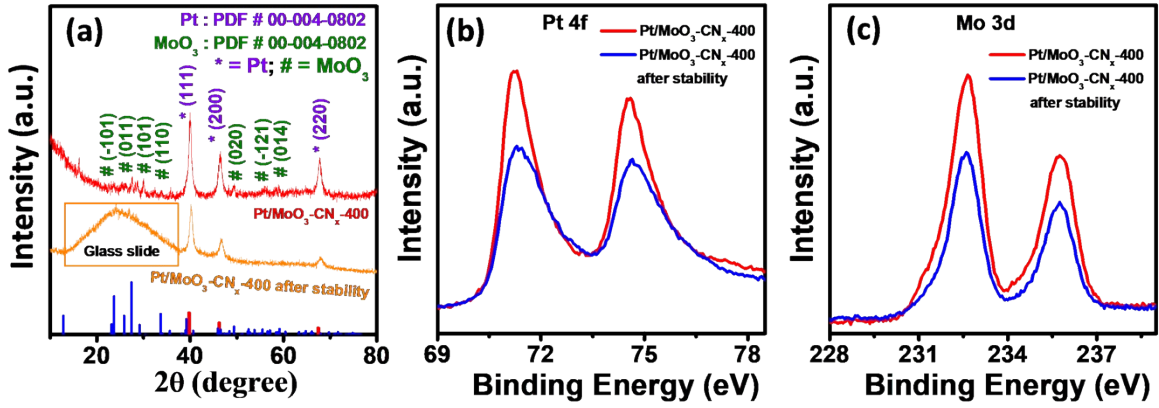


**Figure S6.** (a) p-XRD pattern of Pt/MoO<sub>3</sub>-CN<sub>x</sub>-400 after stability; (b, c) comparison of Pt 4f and Mo 3d XPS data of Pt/MoO<sub>3</sub>-CN<sub>x</sub>-400 after and before the stability test. (d-f) TEM images, (g) HR-TEM image (Inset: SAED image of Pt/MoO<sub>3</sub>-CN<sub>x</sub>-400 after stability).

### **Faradaic efficiency measurements:**

In the water electrolysis process, to quantify the H<sub>2</sub> gases produced, Gas chromatography technique is used to measure the faradic efficiency. A 250 ml five-neck sealed glass cell was used to measure the amount of H<sub>2</sub>. The glass cell has purged with Ar (99.9%) for 2 hours before starting the experiment. The electrolysis was performed with Pt/MoO<sub>3</sub>-CN<sub>x</sub>-400 modified titanium foil electrode (1 cm<sup>2</sup> surface area) as a working electrode, whereas a platinum electrode and Ag/AgCl in 3 M KCl was used as counter and reference electrode. The catalyst loading on the electrode surface was 0.067 mg.cm<sup>-2</sup>. The chronopotentiometry experiment was performed with Pt/MoO<sub>3</sub>-CN<sub>x</sub>-400 modified working electrode at the current density of 10 mA.cm<sup>-2</sup> and at different time interval gas was analyzed with GC instrument (Thermo scientific, Model: Trace 1110) with thermal conductive detector (TCD) and argon as carrier gas.

$$\begin{aligned} & \textit{The Faradic efficiency (\%)} \\ & = \frac{\textit{(number of moles of gas produced experimentally for a certain)}}{\textit{Theoretically calculated gas production (in mole) for the sa}} \end{aligned}$$

The theoretical amount of gas (H<sub>2</sub>) was calculated from accumulated charge during galvanostatic electrolysis by assuming 100% faradic efficiency.

$$\textit{Theoretical amount (n in mole) of gas (H}_2\text{)} = Q / (n * F) = (I * t) / (n * F)$$

Where I is the current in Amp, t is time in sec, n is the number of electrons which is 2 for HER and F is the Faraday constant (96485.3 C.mol<sup>-1</sup>).

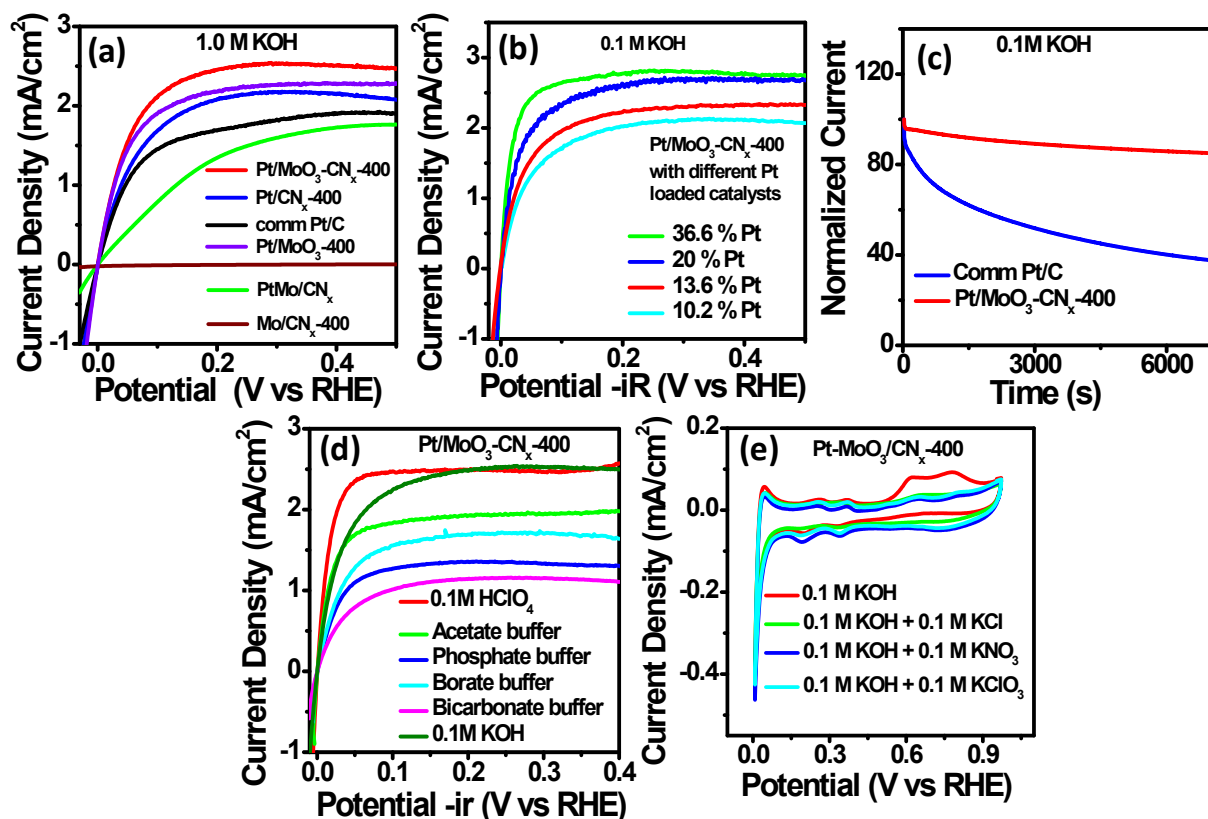


**Figure S7.** (a) Non-iR-corrected HOR plots of Pt/MoO<sub>3</sub>-CN<sub>x</sub>-400, Pt/CN<sub>x</sub>-400, Pt/MoO<sub>3</sub>-400, Comm Pt/C, Mo/CN<sub>x</sub>-400, and PtMo/CN<sub>x</sub> in 0.1 M KOH; (b) HOR of Pt/MoO<sub>3</sub>-CN<sub>x</sub>-400 with different Pt loaded catalysts. (c) HOR stability test of Pt/MoO<sub>3</sub>-CN<sub>x</sub>-400, and commercial Pt/C in presence of nafion binder. (d) HOR polarization curves of Pt/MoO<sub>3</sub>-CN<sub>x</sub>-400 at different pH (buffer) medium; (e) Comparison of CV plots of Pt/MoO<sub>3</sub>-CN<sub>x</sub>-400 on 0.1 M KOH solution containing same amount of different salts.

Catalyst	Solution	Exchange Current Density (mA/cm <sup>2</sup> )	Anodic exchange coefficient ( $\alpha_a$ )	Mass-specific exchange current density (mA/mg <sub>Pt</sub> )	Surface-specific exchange current density (mA/cm <sup>2</sup> <sub>Pt</sub> )	Mass activity at 0.4 V (RHE) (mA/mg <sub>Pt</sub> )
<b>Pt/MoO<sub>3</sub>-CN<sub>x</sub>-400</b>	0.1 M KOH	2.58	0.51	505.7	1.198	490
<b>Pt/MoO<sub>3</sub>-400</b>	0.1 M KOH	2.18	0.51	427.3	1.01	447.9
<b>PtMo/CN<sub>x</sub></b>	0.1 M KOH	0.27	0.5	52	0.264	339.1
<b>Pt/CN<sub>x</sub>-400</b>	0.1 M KOH	1.54	0.51	301.8	0.73	421.4
<b>Comm Pt/C</b>	0.1 M KOH	1.25	0.51	245	0.679	374

**Table S4.** Comparison of HOR activity parameters of Pt/MoO<sub>3</sub>-CN<sub>x</sub>-400 with other catalysts in 0.1 M KOH.

**Table S5:** Comparison of HOR activity of Pt/MoO<sub>3</sub>-CN<sub>x</sub>-400 catalyst in base with other reported catalysts.

Catalyst	Electrolyte	Loading ( $\mu\text{g}/\text{cm}^2$ )	$J_{0,m}$ ( $\text{mA}/\text{mg}_{\text{metal}}$ )	References
Pd/SnO <sub>2</sub> /MOFDC	0.1 M KOH	19.9	114.7	ChemElectroChem 2020, 7, 4562–4571
Commercial Pt	0.1 M NaOH	10	60	J. Chem. Soc. Faraday Trans. 1996, 92, 3719–3725.
Ni@NC/PEI-XC	0.1 M KOH		7.84	ACS Catal. 2021, 11, 12, 7422–7428
Pt <sub>7</sub> Ru <sub>3</sub>	0.1 M KOH	20	49	ACS Catal. 2016, 6, 3895–3908
Ir/O-MoO <sub>2</sub>	0.1 M KOH		45.7	ACS Catal. 2021, 11, 24, 14932–14940
Ir/Mo-MoO <sub>2</sub>	0.1 M KOH		44.0	ACS Catal. 2021, 11, 24, 14932–14940
Acid treatment-PtNi/C	0.1 M KOH	10	474	J. Am. Chem. Soc. 2017, 139, 5156–5163
Ru/Meso C	0.1 M KOH	25.4	540	J. Power Sources 2020, 461, 228147
Pt/Au/C	0.1 M KOH	7	30	ChemElectroChem. 2014, 1, 2058–2063
Ru-Ir/C-60	0.1 M KOH	10	400	ACS Catal. 2020, 10, 4608-4616
PtNb/NbO <sub>x</sub> -C	0.1 M KOH	20	360	ACS Catal. 2017, 7, 4936–4946
Pt/C	0.1 M KOH		203	Small <b>2019</b> , 15, 1903057
Ru <sub>0.5</sub> Co <sub>0.5</sub> /C	0.1 M KOH	14	110	ACS Catal. 2020, 10, 4608-4616
Ru <sub>0.7</sub> Ni <sub>0.3</sub> /C		14	140	
Pd/C-300°C	0.1 M KOH	5	40	J. Electrochem. Soc. 2016, 163, F499–F506
P-Ru/C	0.1 M KOH	6.06	430	ACS Catal. 2020, 10, 11751–11757
Pt/Cu NWs	0.1 M KOH	16	650	J. Am. Chem. Soc. 2013, 135, 13473–13478
Ru <sub>0.20</sub> Pd <sub>0.80</sub> /C	0.1 M KOH	7.06	148	J. Phys. Chem. C 2015, 119, 13481-13487
Pd NTs(Cu)	0.1 M KOH	100	60	J. Am. Chem. Soc. 2013, 135, 36, 13473–13478
Ru <sub>0.20</sub> Pt <sub>0.80</sub>	0.1 M KOH	7.09	696	J. Phys. Chem. C 2015, 119, 13481–13487
PtRu/Mo <sub>2</sub> C–TaC	0.1 M KOH	13	403 ± 25	ACS Catal. 2021, 11, 932–947
(Pt <sub>0.9</sub> Pd <sub>0.1</sub> ) <sub>3</sub> Fe/C	0.1 M KOH	5	330	ACS Catal. 2020, 10, 15207-15216
Ru/C	0.1 M KOH	10	82	Sci. Adv. 2016, 2, e1501602
Commercial Pd/C	0.1 M KOH	20	31	Sci. Adv. 2016, 2, e1501602.
<b>Pt/MoO<sub>3</sub>-CN<sub>x</sub>-400</b>	<b>0.1 M KOH</b>	<b>5.06</b> ( $\mu\text{g}_{\text{Pt}}/\text{cm}^2$ )	<b>505.7</b>	<b>This work</b>

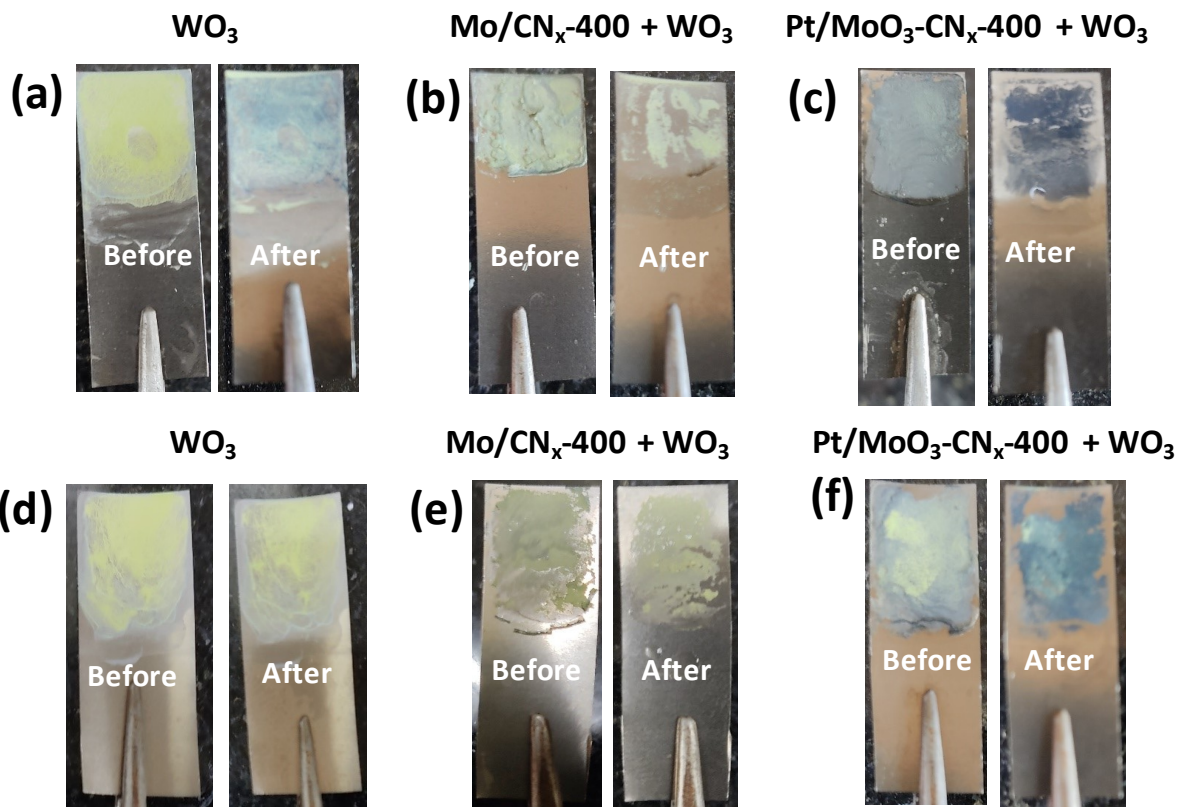


**Figure S8.** (a) Color change photographs of pristine  $\text{WO}_3$  film before and after HER on-titanium foil electrode. (b) Color change photographs of  $\text{Mo}/\text{CN}_x\text{-400} + \text{WO}_3$  film before and after HER on-titanium foil electrode, (c) color change photographs of  $\text{Pt}/\text{MoO}_3\text{-CN}_x\text{-400} + \text{WO}_3$  film before and after HER on-titanium foil electrode. (d) Color change photographs of pristine  $\text{WO}_3$  film before and after HOR on-titanium foil electrode. (e) Color change photographs of  $\text{Mo}/\text{CN}_x\text{-400} + \text{WO}_3$  film before and after HOR on-titanium foil electrode, (f) color change photographs of  $\text{Pt}/\text{MoO}_3\text{-CN}_x\text{-400} + \text{WO}_3$  film before and after HOR on-titanium foil electrode.

## Density Functional Theory (DFT) Calculations:

### Computational details

The electronic structure of  $\beta$ -MoO<sub>3</sub> (011) phase and Pt cluster have simulated using Vienna Ab initio Simulation Package [VASP],<sup>1-4</sup> under the generalized gradient approximation (GGA) functional with Perdew-Burke-Ernzerh of type exchange correlation potential.<sup>5</sup> In this calculation, initially the monoclinic phase of molybdenum oxide  $\beta$ -MoO<sub>3</sub>,<sup>6</sup> thermodynamically stable below 400K was considered to allow the atomic position to relax within the unit cell by space group P2<sub>1</sub>/C with the lattice constant of  $a = 7.18 \text{ \AA}$ ,  $b = 10.89 \text{ \AA}$ , and  $c = 30.79 \text{ \AA}$ , and  $\alpha = 90^\circ$ ,  $\beta = 132^\circ$ ,  $\gamma = 90^\circ$  have optimized by taking energy cut-off 500 eV. Relaxation was carried out till the force on individual atom is less than 0.01 eV/Å. Further, we used the experimentally observed  $\beta$ -MoO<sub>3</sub> plane for the DFT calculations. To set up the  $\beta$ -MoO<sub>3</sub> (011) slab, relaxed bulk geometry was used and optimized again with more than 20 Å of vacuum for the surface study. The Brillouin zones were sampled using a K point's mesh with Monkhorst-Pack scheme<sup>7</sup> grid of 7x7x1 for optimization. Further to support the kinetics of hydrogen spillover mechanism, the work-function of metal [ $\Phi_1$ ] and metal supported  $\beta$ -MoO<sub>3</sub> [011] surface [ $\Phi_2$ ] was obtained. Adsorption energy of active hydrogen species ( $\Delta G_H \approx 0$ ) on catalyst surface is also calculated.

### Structural evolution

The lattice parameter  $a = 7.12 \text{ \AA}$ ,  $b = 10.90 \text{ \AA}$ , and  $c = 29.49 \text{ \AA}$ , and  $\alpha = 90^\circ$ ,  $\beta = 132^\circ$ ,  $\gamma = 90^\circ$  for energetically optimized monoclinic phase of molybdenum oxide  $\beta$ -MoO<sub>3</sub> showing perfect agreement with previous reported data's<sup>6, 8</sup> assuring the reliability of present methodology. Further to understand the mechanism of hydrogen spillover process through HER,  $\beta$ -MoO<sub>3</sub> [011] surface [which was created by cleaving the relaxed  $\beta$ -MoO<sub>3</sub> unit cell], Pt<sub>4</sub> cluster and Pt<sub>4</sub> supported  $\beta$ -MoO<sub>3</sub> [011] are allow to relaxed again to get minimum energy configuration. Schematic representation of all the optimized structure has shown in figure S9.

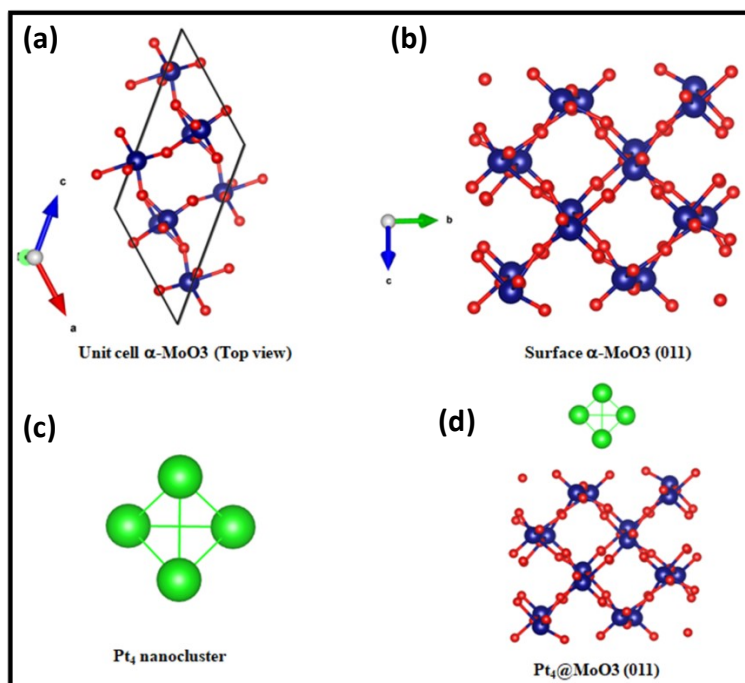


**Figure S9.** Schematic representation of (a) unit cell of bulk  $\beta$ - $\text{MoO}_3$  (top view) (b) Surface  $\beta$ - $\text{MoO}_3$ -011 (c)  $\text{Pt}_4$  cluster and (d)  $\text{Pt}_4$  cluster on surface of  $\text{MoO}_3$  (011). [Blue, red and green colour showing Mo, O, and Pt atoms respectively].

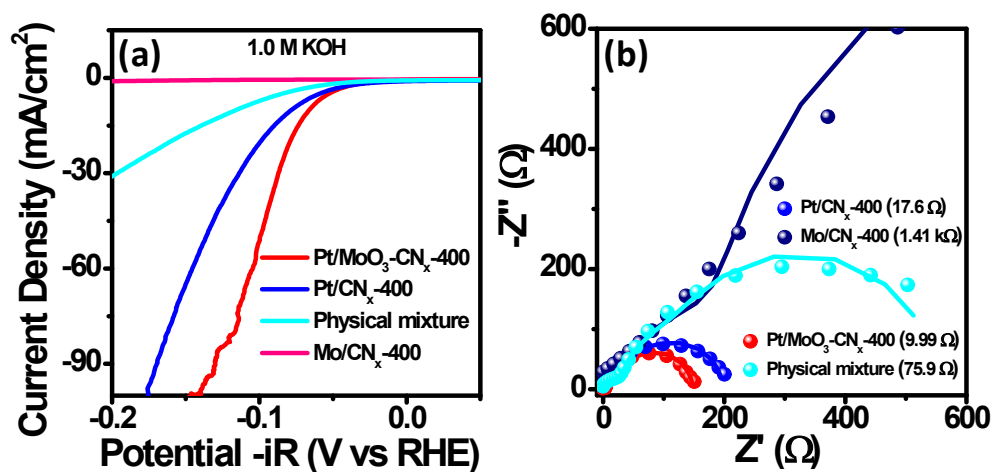


**Figure S10.** (a, b) HER and nyquist plots of Pt/ $\text{MoO}_3$ - $\text{CN}_x$ -400, Pt/ $\text{CN}_x$ -400, Mo/ $\text{CN}_x$ -400, and physical mixture.

## References:

- (1) Kresse, G.; Hafner, J. Ab initio molecular dynamics for liquid metals. *Physical Review B* **1993**, *47* (1), 558-561. DOI: 10.1103/PhysRevB.47.558.
- (2) Kresse, G.; Hafner, J. Ab initio molecular-dynamics simulation of the liquid-metal--amorphous-semiconductor transition in germanium. *Physical Review B* **1994**, *49* (20), 14251-14269. DOI: 10.1103/PhysRevB.49.14251.
- (3) Kresse, G.; Furthmüller, J. Efficiency of ab-initio total energy calculations for metals and semiconductors using a plane-wave basis set. *Computational Materials Science* **1996**, *6* (1), 15-50. DOI: [https://doi.org/10.1016/0927-0256\(96\)00008-0](https://doi.org/10.1016/0927-0256(96)00008-0).
- (4) Kresse, G.; Furthmüller, J. Efficient iterative schemes for ab initio total-energy calculations using a plane-wave basis set. *Physical Review B* **1996**, *54* (16), 11169-11186. DOI: 10.1103/PhysRevB.54.11169.
- (5) Perdew, J. P.; Burke, K.; Ernzerhof, M. Generalized Gradient Approximation Made Simple. *Physical Review Letters* **1996**, *77* (18), 3865-3868. DOI: 10.1103/PhysRevLett.77.3865.
- (6) Parise, J. B.; McCarron, E. M.; Sleight, A. W. A new modification of ReO<sub>3</sub>-type MoO<sub>3</sub> and the deuterated intercalation compound from which it is derived: D<sub>0.99</sub>M<sub>0</sub>O<sub>3</sub>. *Materials Research Bulletin* **1987**, *22* (6), 803-811. DOI: [https://doi.org/10.1016/0025-5408\(87\)90035-3](https://doi.org/10.1016/0025-5408(87)90035-3).
- (7) Wiedenmann, A.; Rossat-Mignod, J.; Louisy, A.; Brec, R.; Rouxel, J. Neutron diffraction study of the layered compounds MnPSe<sub>3</sub> and FePSe<sub>3</sub>. *Solid State Communications* **1981**, *40* (12), 1067-1072. DOI: [https://doi.org/10.1016/0038-1098\(81\)90253-2](https://doi.org/10.1016/0038-1098(81)90253-2).
- (8) Divigalpitiya, W. M. R.; Frindt, R. F.; Morrison, S. R. Oriented films of molybdenum trioxide. *Thin Solid Films* **1990**, *188* (1), 173-179. DOI: [https://doi.org/10.1016/0040-6090\(90\)90203-P](https://doi.org/10.1016/0040-6090(90)90203-P).